AD-A058 276 MINNESOTA UNIV MINNEAPOLIS DEPT OF AEROSPACE ENGINE--ETC F/G 20/11
STRUCTURAL INELASTICITY XXII. A FINITE-ELEMENT MODEL FOR PLANE---ETC(U)
JUN 78 P G HODGE, H M VAN RIJ N00014-75-C-0177

UNCLASSIFIED AEM-H1-22 NL

1 OF 1
AD
A058276

END
DATE
FILMED
10-78
DDC

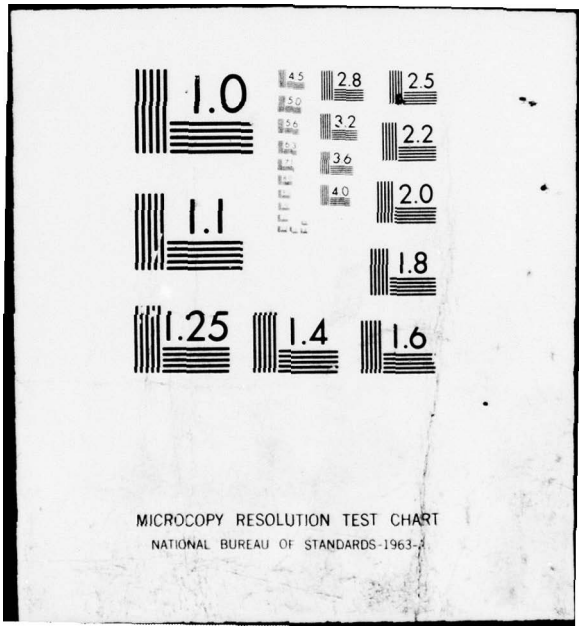
1.0
1.1
1.25
1.4
1.6
1.8
2.0
2.2
2.5
2.8
3.2
3.6
4.0
4.5
5.0
5.6
MICROCOPY RESOLUTION TEST CHART
NATIONAL BUREAU OF STANDARDS-1963-A

(14) Report AEM-H1-22

M64575

LEVEL II

(12)

(6) STRUCTURAL INELASTICITY XXII

M40176

A Finite-Element Model For Plane-Strain Plasticity

(10) Philip G. Hodge, Jr. / Professor of Mechanics

and

Hendrik M. Van Rij / Research Assistant

Department of Aerospace Engineering and Mechanics
University of Minnesota
Minneapolis, Minnesota 55455

(12) 15 p.

(11) June 1978

(15) N00014-75-C-0177

(9) Technical Report

~~Qualified requesters may obtain copies of this report from DDC~~

Prepared for

OFFICE OF NAVAL RESEARCH
Arlington, VA 22217

OFFICE OF NAVAL RESEARCH
Chicago Branch Office
536 South Clark St.
Chicago, IL 60605

405395

15

SECURITY CLASSIFICATION OF THIS PAGE (When Data Entered)

REPORT DOCUMENTATION PAGE

READ INSTRUCTIONS BEFORE COMPLETING FORM

1. REPORT NUMBER: AEM-H1-22	2. GOVT ACCESSION NO.
3. RECIPIENT'S CATALOG NUMBER	
4. TITLE (and Subtitle): STRUCTURAL INELASTICITY XXII "A Finite-Element Model For Plane-Strain Plasticity"	5. TYPE OF REPORT & PERIOD COVERED: Technical Report
	6. PERFORMING ORG. REPORT NUMBER
7. AUTHOR(s): Philip G. Hodge, Jr., Professor of Mechanics Hendrik Van Rij, Research Assistant	8. CONTRACT OR GRANT NUMBER(s): N14-75-C-0177
9. PERFORMING ORGANIZATION NAME AND ADDRESS: University of Minnesota Minneapolis, MN 55455	10. PROGRAM ELEMENT, PROJECT, TASK AREA & WORK UNIT NUMBERS: NR 064-429
11. CONTROLLING OFFICE NAME AND ADDRESS: OFFICE OF NAVAL RESEARCH Arlington, VA 22217	12. REPORT DATE: June 1978
	13. NUMBER OF PAGES: 27
14. MONITORING AGENCY NAME & ADDRESS(if different from Controlling Office): OFFICE OF NAVAL RESEARCH Chicago Branch Office 536 South Clark Street Chicago, IL 60605	15. SECURITY CLASS. (of this report): unclassified
	15a. DECLASSIFICATION/DOWNGRADING SCHEDULE

16. DISTRIBUTION STATEMENT (of this Report)

~~Qualified requesters may obtain copies of this report from DDC~~

17. DISTRIBUTION STATEMENT (of the abstract entered in Block 20, if different from Report)

18. SUPPLEMENTARY NOTES

19. KEY WORDS (Continue on reverse side if necessary and identify by block number)

Plasticity, perfectly-plastic, finite-elements, plane strain, Prandtl punch, slip, velocity discontinuities, combined-finite-element-model.

20. ABSTRACT (Continue on reverse side if necessary and identify by block number)

A finite-element model is proposed which allows for both straining within each element and slip between two elements. Basic equations are derived and are shown to almost completely uncouple into two constituent components: the conventional finite-element equations for continuous displacement fields and the "slip" equations which were recently derived for a model based on slipping of rigid triangles. The model is applied to the Prandtl punch problem and is shown to combine the best features of its two constituents.

DD FORM 1 JAN 73 1473 EDITION OF 1 NOV 65 IS OBSOLETE
S/N 0102-014-6601

SECURITY CLASSIFICATION OF THIS PAGE (When Data Entered)

A Finite-Element for Plane-Strain Plasticity

1. Introduction. In an earlier paper [1]* we pointed out that classical finite element methods suffer from two potential drawbacks when applied to plane-strain problems of contained flow of an elastic/perfectly-plastic material. On the one hand, plastic strain increments are incompressible, a constraint which greatly reduces the number of degrees of freedom in a finite element model. Secondly, some continuum solutions of plasticity problems are known to exhibit discontinuities of tangential velocity across certain boundarys, and classical models cannot handle this feature.

In [1] we proposed a "slip model" which consisted of rigid triangular elements which were free to slide but not separate. Applied to a particular example, the slip model predicted good approximations to the yield-point load, collapse mechanism, and shape of the elastic displacement field. However, all results were obtained in terms of a fictitious elastic modulus which is essentially unknowable.

The present paper is concerned with a "combined model" which apparently has all of the advantages and none of the drawbacks of the classical and slip models taken separately. Further, the computations essentially reduce to a sequence of solutions for classical models and slip models so that the large body of knowledge available for the elastic/plastic classical model can be applied immediately, as can the experience gained in [1] with the slip model.

*Numbers in brackets refer to the references collected at the end of the paper.

All three models are based on triangular elements. For simplicity of exposition and application we shall consider the regular array of right-isosocles triangular elements shown in Fig. 1. The kinematics of the classical model [2] are defined by the dimensionless nodal displacements (u_k, v_k). These displacements define a continuous, piecewise differentiable displacement field and a piece-wise constant strain field over the entire domain. Figure 2 shows the basic unit mechanisms u_k associated with a "small node" (Fig. 2a) and "large node" (Fig. 2b); the v_k mechanisms are similar.

As shown in [1], the kinematics of the slip model are defined by nodal rotations θ_k defined in Fig. 3. The resulting deformation field consists of infinitesimal rigid-body motions of the triangles accompanied by slip of one triangle relative to another.

The proposed combined model has three degrees of freedom at each interior node: a horizontal displacement u_k defined in Fig 2, a similar vertical displacement v_k, and a rotation θ_k defined in Fig. 3. We recall that in the classical model u_k and v_k can also be interpreted as the actual motion of node k. However, in the slip and combined models the rotation θ_k gives a different motion to each vertex at a node, so that the concept of "nodal displacement" has no direct physical significance.

The kinematics of the combined model are fully defined by Figs. 2 and 3; obviously they are the sum of the kinematics of the classical and slip models and there is no coupling of the two models.

The statics of each model can be obtained from Figs. 2 and 3 and the Principle of Virtual Work. If there are no body forces, then it is evident that the resulting static equations for each interior node will be homogeneous and linear, and that the combined model is simply the sum of the other two.

It remains then, to consider the constitutive equations and the boundary conditions, and we will do that in Secs. 2 and 3, respectively. Section 2 will also list generic kinematic and static equations. Then in Sec. 4 we will examine in detail a specific boundary-value problem in order to clearly indicate the character of the proposed model, with particular reference to the close relation between it and the classical and slip models for the same problem. Section 5 will apply the model to an approximation to the Prandtl punch problem [3, 4]. The paper will conclude with a discussion of the merits of the model.

2. Basic equations. We begin by reviewing the well-known equations for the classical model, follow with a summary of the slip-model equations from [1], and conclude by demonstrating that the slip-model constitutive equations are the only ones which must be modified before these equations can be applied to the combined model.

For the classical model the generalized displacements are the dimensionless nodal displacements

$$u_k = U_k/\ell \qquad v_k = V_k/\ell \tag{1}$$

where ℓ is the length of the triangle hypotenuse. These displacements determine a unique continuous piecewise-linear

displacement field which leads to piecewise-constant strains. Taking these as generalized strains ε_x^{α}, ε_y^{α}, γ_{xy}^{α}, we obtain for triangle ADB (triangle 1) in Fig. 2a,

$$\varepsilon_x^{1} = u_B-u_A \qquad \varepsilon_y^{1} = V_A+V_B-2v_D \qquad \gamma_{xy}^{1}=u_A+u_B-2u_D+V_B-V_A \tag{2}$$

with similar expressions for the other elements.

Generalized stresses will be defined by

$$\sigma_x^{\alpha} = \frac{4}{\ell^2 k} \int_{A^{\alpha}} \sigma_x(x,y)\,dA \tag{3}$$

etc. where k is the yield stress in shear. For any reasonable homogeneous material, constant strains will produce constant stresses so that (3) reduces to

$$(\sigma_x^{\alpha}, \sigma_y^{\alpha}, \tau_{xy}^{\alpha}) = (1/k)(\sigma_x, \sigma_y, \tau_{xy}) \tag{4}$$

If point D is the only node with a non-zero displacement in Fig. 2a, then the internal work done in triangle ABD is

$$W_{int} = \int_{ABD} (\sigma_x\varepsilon_x+\sigma_y\varepsilon_y+\tau_{xy}\gamma_{xy})\,dA=(k\ell^2/2)(-v_D\sigma_y^{1}-u_D\tau_{xy}^{1}) \tag{5}$$

The total internal work done by a motion of point D is

$$W_{int}=(k\ell^2/2)\,[u_D(-\sigma_x^{2}+\sigma_x^{4}-\tau_{xy}^{1}+\tau_{xy}^{3})+v_D(-\sigma_y^{1}+\sigma_y^{3}-\tau_{xy}^{2}+\tau_{xy}^{4})] \tag{6}$$

If there is no force applied to node D, the external work must vanish for all choices of u_D and v_D, hence we obtain the linear homogeneous static equations

$$(\sigma_x^{2}-\sigma_x^{4}) + (\tau_{xy}^{1}-\tau_{xy}^{3}) = 0 \tag{7a}$$

$$(\tau_{xy}^{2}-\tau_{xy}^{4}) + (\sigma_y^{1}-\sigma_y^{3}) = 0 \tag{7b}$$

associated with a generic small node. Similarly, at a large node, Fig. 2b, we are led to

$$(\sigma_x^{\,1}+\sigma_x^{\,2}+\sigma_x^{\,3}+\sigma_x^{\,4}) - (\sigma_x^{\,5}+\sigma_x^{\,6}+\sigma_x^{\,7}+\sigma_x^{\,8})$$
$$+ (\tau_{xy}^{\,7}+\tau_{xy}^{\,8}+\tau_{xy}^{\,1}+\tau_{xy}^{\,2}) - (\tau_{xy}^{\,3}+\tau_{xy}^{\,4}+\tau_{xy}^{\,5}+\tau_{xy}^{\,6}) = 0 \qquad (7c)$$

$$(\tau_{xy}^{\,1}+\tau_{xy}^{\,2}+\tau_{xy}^{\,3}+\tau_{xy}^{\,4}) - (\tau_{xy}^{\,5}+\tau_{xy}^{\,6}+\tau_{xy}^{\,7}+\tau_{xy}^{\,8})$$
$$+ (\sigma_y^{\,7}+\sigma_y^{\,8}+\sigma_y^{\,1}+\sigma_y^{\,2}) - (\sigma_y^{\,3}+\sigma_y^{\,4}+\sigma_y^{\,5}+\sigma_y^{\,6}) = 0 \qquad (7d)$$

We consider an elastic/perfectly-plastic material in plane strain. In each element the stresses and strains will be constant, so that the constitutive equations relating the generalized stresses and strains for element α are trivially derived from those for the continuum:

$$f^\alpha = (\sigma_x^{\,\alpha}-\sigma_y^{\,\alpha})^2/4 + (\tau_{xy}^{\,\alpha})^2 \le 1 \qquad \dot\lambda^\alpha \ge 0$$

$$\dot\sigma_x^{\,\alpha} = 2(G/k)[\dot\varepsilon_x^{\,\alpha}+\nu(\dot\varepsilon_x^{\,\alpha}+\dot\varepsilon_y^{\,\alpha})/(1-2\nu)] - \dot\lambda^\alpha(\sigma_x^{\,\alpha}-\sigma_y^{\,\alpha})/2$$

$$\dot\sigma_y^{\,\alpha} = 2(G/k)[\dot\varepsilon_y^{\,\alpha}+\nu(\dot\varepsilon_x^{\,\alpha}+\dot\varepsilon_y^{\,\alpha})/(1-2\nu)] - \dot\lambda^\alpha(\sigma_y^{\,\alpha}-\sigma_x^{\,\alpha})/2$$

$$\dot\tau_{xy}^{\,\alpha} = (G/k)\dot\gamma_{xy}^{\,\alpha} - 2\dot\lambda^\alpha\tau_{xy}^{\,\alpha}$$

IF $f^\alpha < 1$ OR $\dot f^\alpha < 0$ THEN $\dot\lambda^\alpha = 0$

ELSE $\dot\lambda^\alpha = (G/2k)[\sigma_x^{\,\alpha}-\sigma_y^{\,\alpha})(\dot\varepsilon_x^{\,\alpha}-\dot\varepsilon_y^{\,\alpha}) + \tau_{xy}^{\,\alpha}\dot\gamma_{xy}^{\,\alpha}]$ (8)

For the slip model, the dimensionless generalized displacement at nodes D and G in Figs. 3a and 3b, respectively, is

$$\theta_D = d/\ell \qquad \theta_G = d/\ell \qquad (9)$$

A dimensionless generalized strain ω is defined for a generic edge PQ by

$$\omega_{PQ} = d_{PQ}\,\ell_{PQ}/\ell^2 \qquad (10)$$

where d_{PQ} is the relative motion of the two triangles along PQ, defined as positive clockwise. As shown in [1], generalized strains are defined for each horizontal and vertical edge between nodes, but a single generalized strain is defined for each diagonal of a square. Thus, the only non-zero strains associated with the elementary mechanisms in Figs. 3a and 3b, respectively, are

$$\omega_{FG} = \omega_{GB} = \omega_{BA} = \omega_{AF} = \theta_D \qquad \omega_{AG} = \omega_{BF} = -2\theta_D \qquad (11a)$$

$$\omega_{FL} = \omega_{LH} = \omega_{HB} = \omega_{BF} = -\omega_{FG} = -\omega_{LG} = -\omega_{HG} = -\omega_{BG} = \theta_B \qquad (11b)$$

Generalized strains may be related to continuum strains by regarding the edge as a rectangular domain of small thickness $\ell\delta$. In a generic edge PQ the only non-zero strain is

$$\gamma_{xy} = \omega_{PQ}\,\ell/(\ell_{PQ}\delta) \qquad (12)$$

Since γ_{xy} is constant, the only non-zero continuum stress is the constant τ_{xy} and we define a generalized stress by

$$\tau_{PQ} = \lim_{\delta\to 0} \int_A \frac{\tau_{xy}\,dA}{k\ell\,\ell_{PQ}\delta} = \frac{\tau_{xy}}{k} \qquad (13)$$

Then the internal work done in edge PQ is

$$W_{int}^{\,PQ} = k\ell^2\,\tau_{PQ}\omega_{PQ} \qquad (14)$$

Therefore, if no external work is done in the mechanism motions in Fig. 3, the linear, homogeneous static equations are easily obtained:

$$\tau_{FG} + \tau_{GB} + \tau_{BA} + \tau_{AF} - 2\tau_{AG} - 2\tau_{BF} = 0 \qquad (15a)$$

$$\tau_{FL} + \tau_{LH} + \tau_{HB} + \tau_{BF} - \tau_{FG} - \tau_{LG} - \tau_{HG} - \tau_{BG} = 0 \qquad (15b)$$

Formal combination of the Prandtl-Reuss flow law for pure shear with Eqs. (12) and (13) leads to the constitutive equation for edge PQ:

$$\tau_{PQ}^2 \leq 1 \tag{16a}$$

$$\text{IF } \tau_{PQ}^2 < 1 \text{ OR } \tau_{PQ}\dot{\tau}_{PQ} < 0 \tag{16b}$$

$$\text{THEN } \dot{\tau}_{PQ} = (G\ell/k\ell_{PQ}\delta)\dot{\omega}_{PQ} \tag{16c}$$

$$\text{ELSE } \dot{\tau}_{PQ} = 0 \tag{16d}$$

Now, Eq. (16c) is not usable as written, since it contains the "thickness" δ of the edge - which must tend to zero. For the slip model this dilemma is resolved by defining a "slip modulus".

$$G' = G/\delta \tag{17}$$

As shown in [1], this procedure enables us to obtain complete elastic/plastic stress distributions and to obtain displacement fields in terms of the unknown (and unknowable) constant G'.

However, for the combined model considered here, the shear modulus G is necessary for Eqs. (8) to have meaning, and hence it cannot be allowed to tend to zero as is implied by Eq. (17). Therefore, we must resolve our dilemma in a different way by defining new alternative kinematic variables $\bar{\theta}_p$, etc. by

$$d_{PQ} = \bar{d}_{PQ}\delta \quad \omega_{PQ} = \bar{\omega}_{PQ}\delta \quad \theta_P = \bar{\theta}_P\delta \tag{18}$$

Equations (16) then become

$$\tau_{PQ}^2 \leq 1 \tag{19a}$$

$$\text{IF } \tau_{PQ}^2 < 1 \text{ OR } \tau_{PQ}\dot{\tau}_{PQ} < 0 \tag{19b}$$

$$\text{THEN } \dot{\bar{\omega}}_{PQ} = 0 \text{ AND } \dot{\tau}_{PQ} = (G\ell/k\ell_{PQ})\dot{\bar{\omega}}_{PQ} \tag{19c}$$

$$\text{ELSE } \dot{\ell}_{PQ} = 0 \tag{19d}$$

If (19b) is satisfied, there will be no slip. However, in view of Eq. (18), zero slip is compatible with non-zero alternative variables $\bar{\omega}_{PQ}$ so that we still have a meaningful set of slip equations. In particular, $\dot{\tau}_{PQ}$ and hence τ_{PQ} can be determined so that the continued validity of (19b) can be tested. On the other hand, if (19b) is violated, we bypass (19c) to obtain directly the simple (19d). Since this equation gives no kinematic information it is compatible with either zero ω_{PQ} and meaningful $\bar{\omega}_{PQ}$, or with non-zero ω_{PQ} in which case the alternative kinematic variables are discarded. The choice between these two alternatives will depend upon the problem as a whole, and will be discussed in later sections.

With the exception of the above discussion of the constitutive equations, it is clear that the defining equations for the classical and slip parts are independent and hence may be combined for the classical model. Therefore, for the combined model the kinematics are governed by Eqs. (2), (11) and (18), the statics by (7) and (15), and the constitutive behavior by (8) and (19).

3. Boundary value problem. Boundary conditions are most easily discussed in terms of a specific example. To this end we consider the problem shown in Fig. 1. For any of the three models local constitutive equations and strain-displacement equations will exactly match the unknown generalized strains and stresses.

Therefore, in order to balance the total system of equations and unknowns, there must be one equilibrium equation for each generalized displacement.

For the classical model, each of the interior nodes has two displacement unknowns u_i and v_i, and the same number of equations, Eqs. (7). On the boundary, u = 0 for nodes G-M and v = 0 for nodes M-S. The vertical displacements at nodes A-E, H-L, and T-X are not subject to any constraints. Therefore, we can use Eq. (7d) for these 15 additional unknowns, keeping only those stress terms which correspond to triangles in the domain. Similarly, we can modify Eq. (7c) for the 5 unknowns u_N-u_R. The remaining nine nodal displacements are given by

$$u_S = u_T = u_U = u_V = u_W = u_X = u_A = u_0 \qquad v_F = v_G = -v_0 \tag{20}$$

Applying the principle of virtual work to motions defined by u_0 and v_0, respectively, we obtain

$$T_2 = (1/12) \sum_1^6 [-(\sigma_x^{i1}+\sigma_x^{i3}+2\sigma_x^{i4})+(\tau_{xy}^{i1}-\tau_{xy}^{i3})] \tag{21a}$$

$$T_1 = (1/2)\ [-(\tau_{xy}^{71}+\tau_{xy}^{72}+\tau_{xy}^{82}-\tau_{xy}^{84})$$

$$-(\sigma_y^{71}+\sigma_y^{72}+2\sigma_y^{81}+\sigma_y^{82}+\sigma_y^{84})] \tag{21b}$$

where kT_2 and kT_1 are, respectively, the dimensionless forces pushing SA to the right and FG down. If T_2 is given, (21a) is the necessary equation for the additional unknown u_0; if u_0 is given, (21a) defines the necessary force T_2. Similar interpretations apply to T_1 and Eq. (21b).

For the slip model, we first note that if all θ_i were equal, the entire domain would remain unchanged, so that we may arbitrarily

set $\theta_M = 0$. Next, we regard displacement boundary conditions as being applied by fictitious triangles external to the domain. For example, the fictitious triangle above line FG moves down a prescribed distance $v_0\ell$.

The fictitious triangles along MS cannot move vertically, so that $\theta_M = 0$ implies $\theta_N = 0$. By similar arguments we see that all of θ_G-θ_S must vanish. Since $\theta_S = 0$, we must have

$$\theta_T = u_0 \tag{22a}$$

The mechanism motion defined by (22a) would move the fictitious triangle on the TU a distance u_0 to the left. Therefore, to satisfy the boundary condition that it move u_0 to the right we require

$$\theta_U = 2u_0 \tag{22b}$$

Continuing this argument, we see that

$$\theta_V = 3u_0 \quad \theta_W = 4u_0 \quad \theta_X = 5u_0 \quad \theta_A = 6u_0 \tag{22c}$$

Finally, along on the top surface

$$\theta_F = -v_0 \tag{22d}$$

and θ_B-θ_E are four new variables.

As shown in [1] boundary mechanisms are somewhat simpler than interior ones, so that the equilibrium equation for node B is

$$\tau_{AX'} + \tau_{CX'} - \tau_{BX'} = 0$$

with similar expressions for nodes C, D, and E. The mechanism motion for v_0 involves only node F and leads to

$$T_1 = -\tau_{EF'} - \tau_{GF'} + \tau_{FF'} + \tau_{FG/2} \tag{23}$$

whereas the mechanism motion for u_0 involves all of the nodes on the left and leads to

$$T_2 = (1/6)[(\tau_{ST}'+\tau_{UT}'+\tau_{TT}') + 2(\tau_{TU}'+\tau_{VU}'-\tau_{UU}') + 3(\tau_{UV}'+\tau_{WV}'-\tau_{VV}') + 4(\tau_{VW}'+\tau_{XW}'-\tau_{WW}') + 5(\tau_{WX}'+\tau_{AX}'-\tau_{XX}') + 6\tau_{XB}] \quad (23b)$$

As with the classical model, Eqs. (23) may be used to find displacements if forces are given or to define forces for given u_0 and/or v_0.

For the combined model, we must interpret the presribed boundary motions in terms of permissible mechanism motions. However, before doing this, we observe that not all of the generalized displacements in the total domain are independent. As with the slip model, we may arbitrarily set $\theta_M = 0$. Further, we observe from Fig. 3 that the combination of a unit slip mechanism at node D together with large node mechanisms $\theta_A = \theta_B = 2$ has the effect of shifting the square ABGF one unit to the right but leaving it internally undeformed. Applying this same reasoning to the domain in Fig. 1 we see that if $\theta = 0$ along the bottom row, $\theta = 2$ along the row TL of large nodes, $\theta = 4,6,8,10,12$, respectively, along rows UK, VJ, WI, XH, and AG, together with $\theta = 1,3,5,7,9,11$ along the rows of small nodes counting from the bottom moves the entire domain one unit to the right. Superposition of $u_i = -1$ for all nodes would then leave the entire domain unmoved. Therefore, we may arbitrarily set $u_M = 0$. A similar argument applied to vertical motion shows that v_M may also be taken as zero. We note that these three arbitrary conditions

are inherent in our choice of kinematic variables and are not related to a rigid-body motion of the entire domain.

Returning to the problem of Fig. 1, we consider first the motion of triangle 92. The resultant vertical motion of vertices M and N can be written in terms of rotation and vertical mechanism motions of nodes M and N, and must vanish:

$$v_M + (\theta_M-\theta_N)/2 = v_N + (\theta_M-\theta_N)/2 = 0 \quad (24)$$

Since we have set $v_M = \theta_M = 0$, it follows that $v_N = \theta_N = 0$. Similar reasoning along the bottom and right side shows that $\theta_G-\theta_S$, u_G-u_M, and v_M-v_S all vanish.

Since $u = u_0$ on SA, the horizontal displacements of vertices S and T of triangle 64 are given by

$$u_S + (\theta_T-\theta_S)/2 = u_T + (\theta_T-\theta_S)/2 = u_0 \quad (25)$$

whence $u_S = u_T$. Similar reasoning applies all along side SA, and we define a new variable.

$$u_{0c} = u_S = u_T = u_U = u_V = u_W = u_X = u_A \quad (26a)$$

Further, it follows from Eqs. (25), similar equations for triangle 54, and the previous result $\theta_S = 0$ that $\theta_U = 2\theta_T$. We introduce a second new variable u_{0s} and use similar reasoning along all of side SA to show

$$u_{0s} = \theta_T = \theta_U/2 = \theta_V/3 = \theta_W/4 = \theta_X/5 = \theta_A/6 \quad (26b)$$

In terms of these new variables Eqs. (25) and all similar equations for side SA are satisfied by

$$u_{0c} + u_{0s} = u_0 \quad (26c)$$

Similar reasoning applied to FG leads to

$$v_F = v_G = -v_{0c} \qquad \theta_F = -v_{0s} \qquad v_{0c} + v_{0s} = v_0 \tag{27}$$

Examining the boundary value problems for the three models, we see that the combined model equations are the totality of those for the other two models except for the equations based on motions u_0 and v_0. Thus, a combined model problem can be almostly completely uncoupled into separate classical and slip model problems. We shall discuss the details of this phenomenon in the next section.

4. Solution. We consider a specific case of the boundary value problem defined in Fig. 1 where $u_0 = 0$ and v_0 is slowly increased from zero.

For v_0 sufficiently small, all elements will be elastic. Therefore all classical elements will follow the first branch in Eqs. (8) and all slip elements will follow the first in Eqs. (19). Thus, Eq. 19c will lead to the vanishing of all real slip displacements, specifically including u_{0s} and v_{0s}. Therefore, $u_{0c} = 0$ and $v_{0c} = v_0$, and the combined problem is identical to the classical one with prescribed displacement conditions. Therefore, it can be solved without reference to Eqs. (21) which are then available to determine T_1 and T_2. But with T_1 and T_2 known, the remaining combined model equations are identical to those of the slip model with alternative kinematic variables and prescribed loads. Therefore, in the elastic range we can solve the combined model by solving the classical and slip models in order.

Now for some critical value of v_0, some element must reach yield and from here on all equations must be written in rate form.

If a triangle yields we must take the second branch in (8), but the method of analysis remains unchanged. When the first slip element yields, either before or after yielding of any triangle elements, the second branch of Eqs. (19) must be used for that element. However, it is not possible for any one $\dot{\omega}_{PQ}$ to be non-zero, so that we must continue to use the alternative kinematic slip variables. Thus, at this stage also we are in the uncoupled plastic range where the combined model is solved by sequential solution of the classical and slip models.

As v_0 is still further increased, more and more elements will reach yield and require the second branch in Eqs. (8) or (19). Eventually, sufficient slip elements will reach yield so that, if u_{0s} and v_{0s} are both regarded as free variables, a combined mechanism motion of the slip model would be possible. Since all rotation displacements in this motion can be expressed in terms of u_{0s} and v_{0s}, the mechanism will be defined by some relation

$$\alpha\dot{u}_{0s} + \beta\dot{v}_{0s} = 0 \tag{28}$$

where α and β are not both zero. It turns out that no external work is associated with this mechanism, so that

$$6\dot{T}_2\,\dot{u}_{0s} + \dot{T}_1\,\dot{v}_{0s} = 0 \tag{29}$$

hence

$$\alpha\dot{T}_1 - 6\beta\,\dot{T}_2 = 0 \tag{30}$$

For further increase in v_0, the boundary displacements for the classical problem are now defined by

$$\dot{u}_{0c} = -\dot{u}_{0s} \qquad v_{0c} = v_0 - \dot{v}_{0s} \tag{31}$$

Additional equations for the two new unknowns $\dot{u}_{0s}$ and $\dot{v}_{0s}$ are provided by (28) and by the substitution of (21) in (30).

One the classical problem is solved, $\dot{u}_{0s}$ and $\dot{v}_{0s}$ will be known, hence so will those $\dot{\theta}_i$ which are involved in the mechanism. The remainder of the slip model can still be solved in terms of the alternative kinematic variables. In obtaining this solution we can arbitrarily set one of the external alternative kinematic variables equal to zero, say $\dot{\bar{u}}_{0s}$, since the forces will automatically satisfy (30).

Further increase of v_0 will lead to more elements becoming plastic. However, until a second mechanism forms we remain in the partly-coupled plastic range where the two parts are coupled only by Eqs. (28) and (30) and hence may still be solved sequentially.

The next critical value of v_0 occurs when an independent second slip mechanism forms. Now $\dot{u}_{0s}$ and $\dot{v}_{0s}$ are independent variables not subject to (28). Since neither of these independent mechanisms will do net work,

$$\dot{T}_1 = \dot{T}_2 = 0 \tag{32}$$

and we have reached the yield-point load. Further increase in load is impossible for a perfectly-plastic material in equilibrium.

Conceivably, the classical model alone could activate a yield-point mechanism while in the uncoupled range, or a mechanism could be formed in the partly-coupled range; in the examples considered, however, this was never the case.

Three complications to the qualitative description given above may occur. In the first place, even though v_0 increases

monotonically, some elements may unload. Thus, after using the second branch in Eqs. (8) a check must be made that $\dot{\lambda}^\alpha$ is non-negative. Similarly, if (19d) is used, $\dot{\omega}_{PQ}$ or $\dot{\bar{\omega}}_{PQ}$ must have the same sign as τ_{PQ}. Any element or elements where these requirements are not met must be switched to the other branch.

Secondly, the plastic solution to (8) for a triangle should satisfy the non-linear equation $\dot{f} = 0$. Instead, it satisfies a linear condition equivalent to moving along a tangent to the surface $f = 1$, thus resulting in $\dot{f} > 0$. In order to keep the resulting error from growing too large, it is desirable to stop a stage whenever the change in f exceeds, say, 0.001, and to recompute the stress terms that appear in Eqs. (8).

Finally, in some stages a lack of uniqueness occurs for the kinematical slip variables. This phenomenon was found in [1] for the slip model. At least in the uncoupled range, it is less disturbing here than in [1], since it involves only the alternative kinematic slip variables and the true slip remains uniquely zero.

We shall comment on all three of these complications more fully in relation to the example in the next section.

5. Example. A computer program was written to implement the three models and was used to solve the problem illustrated in Fig. 1 with $u_0 = 0$. An elastic/perfectly plastic material is placed in a perfectly lubricated box and indented with a rigid punch. This problem which was considered in Sec. 4 is a finite domain approximation to the Prandtl problem [3,4] of a rigid rough punch indenting a semi-infinite perfectly-plastic material

under conditions of plane strain. Details of the solution and a discussion of the computer program may be found in [5].

The slip model solution [1] is independent of Poisson's ratio; for the classical and combined model we took $\nu = 0.3$.

The yielding sequence of the edges and the triangles is shown in Fig. 4. In the uncoupled range the classical part of the solution is exactly the same for the classical and combined models. However, the slip part of the solution with the combined model is not identical with that of the slip model [1], since the stress solution interacts with the reaction forces of the classical part, even in the absence of slip. As might be expected, these differences grow as the load increases. A comparison of Fig. 4a and results from [1] shows that the first three edges to yield in the slip model are the first three to yield in the same order in the slip part of the combined model. The first eight edges to yield in the slip model are among the first nine, but in different order, to reach the yield stress in the slip part of the combined model. However, the ninth edge to yield in the slip model is only the 14th to reach yield in the slip part of the combined model, and the tenth yielding edge in the slip model is the 23rd in the slip part of the combined model.

As in the slip model solution, more than one edge may reach yield at the same time, as in stages 72, 73, and 76. In this example we never find two triangles reaching yield at the same time, although the phenomenon could certainly occur. However, at the end of stage 68 we find both one triangle and one edge reaching yield. None of the above coincidences cause any

computational difficulty.

We also find that several stages are ended by an 0.001 increase in f. Specifically, this happens to end stages 19, 25, 29, 34, 38, 47, 50, 55, 57 and 69 in the uncoupled range.

Load deflection curves for the three models are shown in Fig. 5. It is interesting to note that even though edge yielding in the uncoupled range does not influence the load deflection curve, the elastic limit of the combined model occurs at $T_1 = 2.52$, $v_0 = 1.92$ G/k when edge FF' reaches yield, whereas the fully elastic range in the classical model is terminated when triangle 72 yields at $T_1 = 2.76$ and $v_0 = 2.10$ G/k.

At the end of stage 73 we find an undetermined rotation variable in the lower right corner. Although this nonuniqueness of an alternative kinematic variable is a computational nuisance, it does not affect any of the stress variables or real kinematic variables, and does not lead to coupling between the classical and slip parts.

At the end of the stage 76 seven edges yield and produce several independent slip mechanisms of the true kinematic slip variables. However, all mechanisms involve the same motion at the boundaries, and Eqs. (28) and (30) become, respectively,

$$\dot{v}_{0s} = 6\,\dot{u}_{0s} \qquad \dot{T}_1 + \dot{T}_2 = 0 \tag{33}$$

As described in Sec. 4, we enter a new phase of the solution, where we have one interacting force between the classical part and the slip part. As a consequence the loading conditions of the classical part change. This change has a dramatic effect on the behavior of the triangular elements in that more than

half of the elements which were yielding at the end of stage 76 (17 out of 29), now start to unload. These elements are indicated by asterisks in Fig. 4b.

Figure 5 shows that in this phase the load-deflection curve is no longer the same as the classical model due to the slip in the domain. Computation in this phase continues until the end of stage 91 when four simultaneously yielding edges cause limit load conditions. The limit load and the collapse mechanisms are the same as we found in [1] for the Prandtl rough punch with the slip model.

Also shown in Figure 5 is the continuation of the load deflection curve for the classical model up to stage 115 when the load was about 14% above the yield-point load for the combined model. Further computation up to stage 153 increased the load to about 30% above the combined yield-point load and caused plastic flow in more than half the triangles, but still did not produce a yield-point mechanism. This phenomenon will be commented on in the final section.

6. Conclusions. We begin this section by summarizing some of the results for the three different models as applied to the Prandtl punch problem considered in Sec. 5. The classical model provides a well defined elastic solution which agrees well with an analytical solution for a semi-infinite domain obtained by Green and Zerna [6]. Plastic regions develop in what appears to be a reasonable sequence with no unloading up to a load of about 7.25. As shown in [5], the computer program appears to

become unstable above this point, and it does not predict a limit load. However, the theorems of limit analysis may be applied directly to this model [5, Appendix C] and they show that $T_1 = 7.23$ is the true limit load for the model.

The slip model gives only relative displacements, but these agree well with the analytical solution [6]. It predicts a limit load of 6.00, which is a reasonable upper bound on the true value of 5.14 [3,4]. It provides many possible collapse mechanisms, one of which agrees well with the analytical one [1].

The combined model agrees exactly with the classical one up to $T_1 = 5.7$, gives exactly the same collapse load $T_1 = 6.00$ and mechanisms as the slip one, and provides a transition solution between these two which appears reasonable.

Bars with notches in one or both sides and the Prandtl problem with a smooth punch were also considered in [5], with similar results. Based on this limited experience it appears that the combined model gives results which combine the best features of the other two.

The computations were carried out on a CDC Cyber 74. The total CPU times were approximately 30, 80, and 130 seconds for the slip, classical, and combined models, respectively. A more meaningful comparison is the time per degree of freedom which was, respectively, 0.44, 0.55, and 0.62 seconds for the three models. Unquestionably, more efficient programmers could reduce these times substantially, but their relative magnitudes are probably meaningful. Thus, on either a total or degree-of-freedom basis the combined model is the most time consuming. However, in view of the fact that neither the classical nor slip models provide an adequate complete

elastic-plastic history, it is important to note that the combined-model time is only slightly more than the sum of the other two.

References

1. Van Rij, H. and Hodge, P.G., Jr., "A Slip Model for Finite-Element Plasticity", Journal of Applied Mechanics, Vol. 45, 1978, (in press).
2. Turner, M.J., Clough, R.W., Martin, H.C., and Topp, L.J., "Stiffness and Deflection Analysis of Complex Structures", J. Aero. Sci., Vol 23, 1956, pp 805-823.
3. Prandtl, L., "Ueber die Harte plastischer Koerper", Goettinger Nachr, Math-Phys, Kl 1920, 1920, pp 74-85.
4. Prager, W., and Hodge, P.G., Jr., Theory of Perfectly Plastic Solids, Wiley, New York, 1951 (Xerox Univ. Microfilms, OP69234).
5. Van Rij, H. and Hodge, P.G. Jr., "Finite Element Models with Velocity Discontinuities", AEM Report H1-21, University of Minnesota, June, 1978.
6. Green, A.E. and Zerna, W., Theoretical Elasticity, Clarendon, Oxford, 1954.

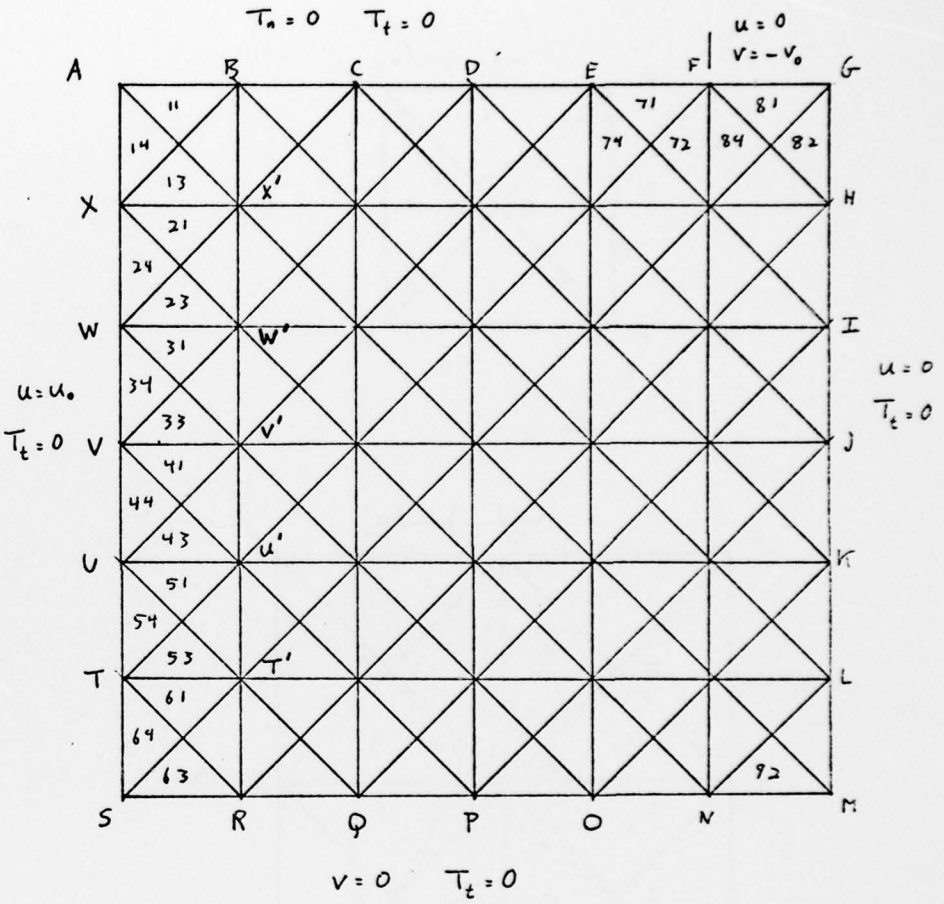

Fig. 1 Finite-element arrangement for Prandtl punch

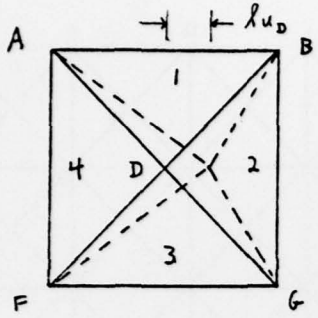

(a)

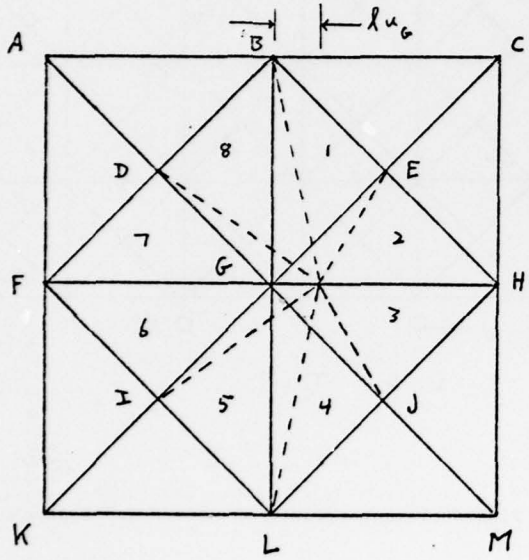

(b)

Fig. 2 Elementary horizontal mechanisms

(a) small node

(b) large node

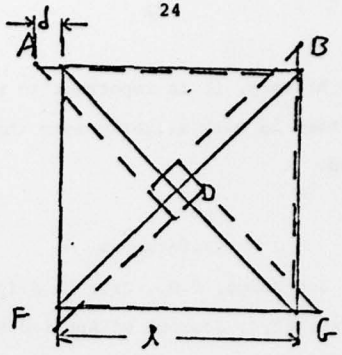

(a)

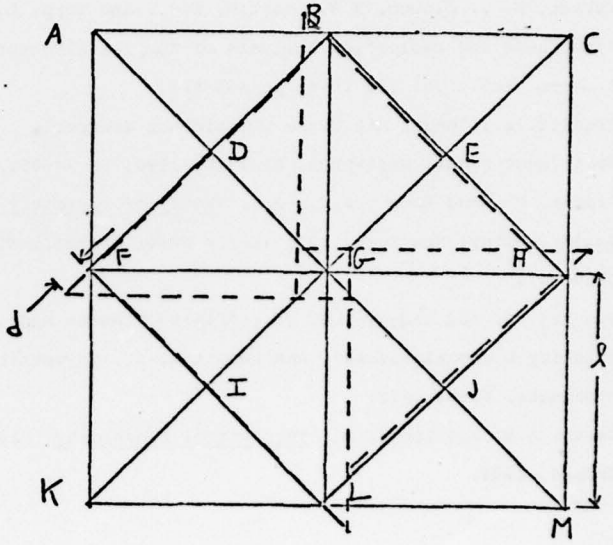

(b)

Fig. 3 Elementary slip mechanism

(a) small node

(b) large node

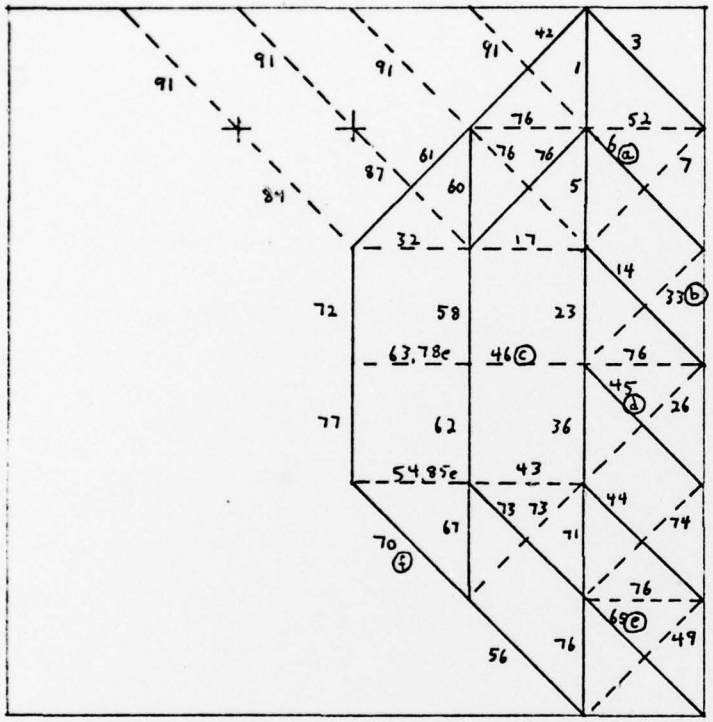

(a)

——— τ=1

- - - - - τ=-1

ⓐ 15e, 20, 44e, 76

ⓑ 55e, 75

ⓒ 63e, 66, 69e

ⓓ 50e, 68

ⓔ 68e, 72

ⓕ 77e, 85

Fig. 4 Yielding sequence for Prandtl punch

(a) edges

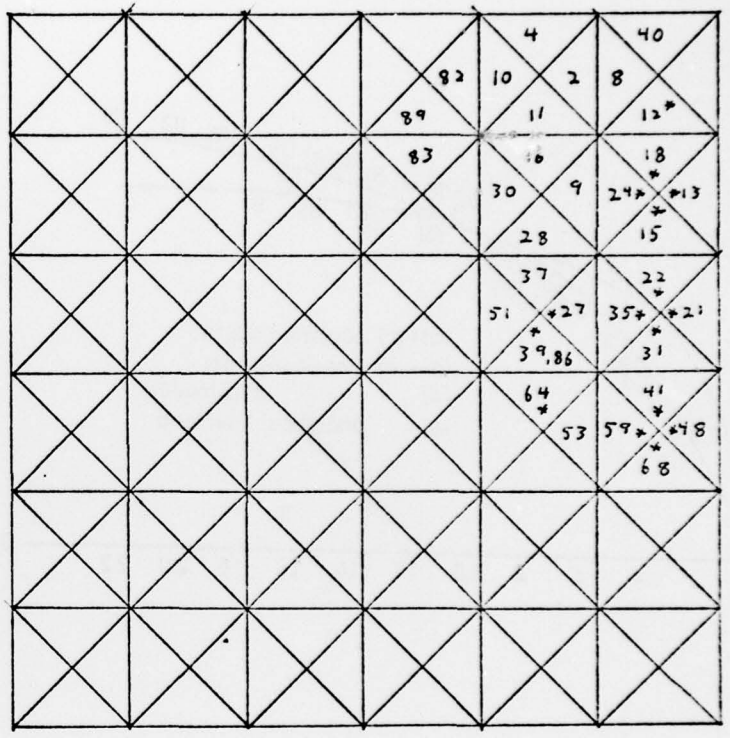

(b)

* Element unloads at end of stage 76

Fig. 4 Yielding sequence for Prandtl punch

(b) triangles

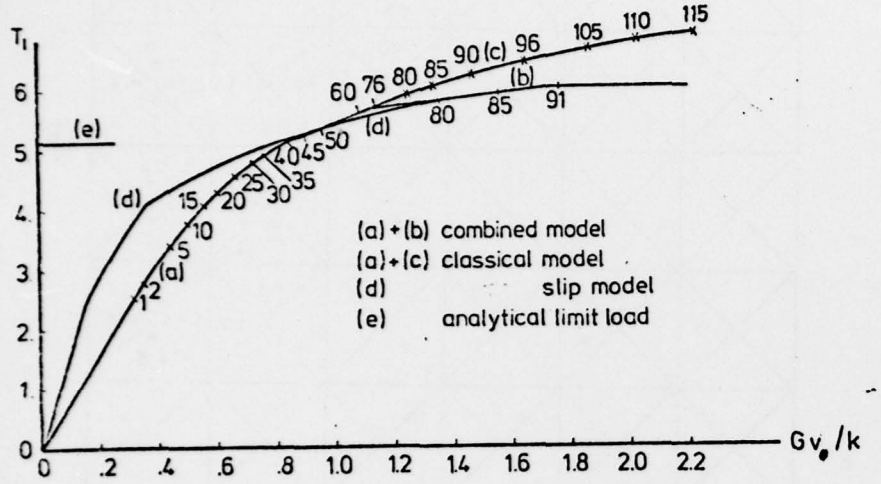

Fig 5 Load-displacement curve for Prandtl punch